Nordic Hydrology, 21, 1990, 65-80

Assessing the Effect of Longitudinal Density Gradient on Estuarine Hydrodynamics

Kolawole O. Aiyesimoju
East Bay Municipal Utility District,
Oakland, CA-94607, USA

If the impact of longitudinal density gradient on the hydrodynamics of estuaries is negligible, then in water quality simulations, the hydrodynamics can be decoupled from the mass transport which would lead to substantial savings in computational time and storage requirements. It is thus important to be able to assess this impact beforehand.

The impact of longitudinal density gradients is evaluated analytically in the context of a one-dimensional wide rectangular channel taking into account the influence of bed slope, bottom friction, type of boundary condition and transient effects. The analysis predicts actual errors that would arise in numerical computations from near exactly in the best cases to within a factor of 6 in the worst cases. It should thus be useful for at least an order of magnitude prediction of the errors that would arise from the neglect of the effect of longitudinal density gradient on estuarine hydrodynamics.

Introduction

Previous work on estuarine hydrodynamics and water quality modeling is numerous and cannot be summarized here. Reviews are given in TRACOR (1971) and Liu and Leendertsee (1978). Most of these previous studies either coupled the hydrodynamics equations and the mass transport equations or decoupled them without examining what should be the determining factor, the impact of longitudinal density gradients. If this impact is negligible, the hydrodynamics can be decoupled from the mass transport which would lead to substantial savings in computational time and storage requirements.

To the knowledge of the writer, the only previous assessments of this impact (Fisher, Nava and Cross 1971, and Dailey and Harleman 1972) were limited to comparing the relative magnitudes of the pressure gradient terms in the momentum conservation equation with and without longitudinal density gradient. The influence that the unsteady nature of estuarine flow, the types of boundary conditions specified, bottom friction and bed slope may have was thus summarily neglected.

An analytical approach which includes these variables will be taken. This will necessitate the adoption of reasonable assumptions to facilitate the analysis without detracting from its essence, which is to provide a decision-making tool as to the desirability of including longitudinal density gradient effects in a given estuarine water quality simulation. A numerical approach will avoid most of these assumptions but the resulting numerical predictive tool cannot be readily made available to others.

Although the analysis done here will be in the context of one-dimensional wide rectangular channels, there is no reason why the conclusions should not remain relevant for channels that are vertically well-mixed in general.

Governing Equations and Assumptions

The field equations describing long wave propagation in a one-dimensional wide rectangular channel in the presence of density gradients are (Aiyesimoju 1986) respectively the mass conservation and momentum conservation equations

$$\frac{\partial}{\partial t}(\rho h) + \frac{\partial}{\partial x}(\rho q) = 0 \tag{1}$$

$$\frac{\partial}{\partial t}(\rho q) + \frac{\partial}{\partial x}\left(\rho \frac{q^2}{h}\right) + gh\frac{\partial}{\partial x}(\rho h) - \frac{gh}{2\rho}(\rho h)\frac{\partial \rho}{\partial x} + \rho g h (S_f - S_0) = 0 \tag{2}$$

where

x	– the longitudinal distance,
t	– time,
$q\ (x, t)$	– the discharge per unit width,
$h\ (x, t)$	– the water depth,
z_b	– the bed elevation with respect to a given datum,
$\varrho(x, t)$	– the water density,
S_f	– the friction slope,
S_o	– the bed slope $-\partial z_b/\partial x$
g	– the gravitational acceleration.

The following assumptions will facilitate the analytical evaluation without detracting from the essence of the analysis; the impact of longitudinal density gradient on estuarine hydrodynamics: 1) Convective acceleration term $\partial/\partial x(\varrho q^2/h)$ is negligible, 2) Variations to still water level $(h\text{-}H)$ are relatively small compared to mean water depth H *i.e.* h/H is close to unity, 3) Longitudinal density variations are sufficiently small that $1/\varrho(\partial\varrho/\partial x)\approx 1/\varrho_f\ \partial\varrho/\partial x$, where ϱ_f is the freshwater density, 4) Friction is linear such that $ghS_f = \mu q$ (the estimation of μ the linear friction coefficient will be discussed later) and 5) Constant bed slope.

Assumptions 1), 2), 4) and 5) have been successfully used in analytical studies (See Dronkers 1964, p 225; Bode and Sobey 1984). Assumption 3) is reasonable since in real estuaries ϱ deviates from ϱ_f by no more than 4% in the worst cases (*e.g.* 2.4% in San Francisco bay and 1.6% in Guayas estuary in Ecuador). A salinity of 40 parts per thousand corresponds to a deviation of about 3.2% at 4° C.

Under the above assumptions, the mass conservation Eq. (1) remains the same and the momentum conservation Eq. (2) can be written as

$$\frac{\partial}{\partial t}(\rho q) + gH\frac{\partial}{\partial x}(\rho h) - \frac{gH}{2\rho_f}(\rho h)\frac{\partial \rho}{\partial x} + \mu\rho q - \rho g H S_0 = 0 \qquad (3)$$

It is more convenient to work in dimensionless terms. Let $x' = x/L,\ t' = t/T$,

$$\rho'(x',t') = \frac{\rho(x,t)}{\rho_f},\quad h'(x',t') = \frac{h(x,t)}{H},\quad q'(x',t') = \frac{q(x,t)L}{gTH^2}$$

and

$$S' = \frac{LS_0}{H}$$

where L is channel length and T is period of wave component being considered. Substituting in Eqs. (1) and (3) gives respectively for mass conservation and momentum conservation

$$\frac{\partial}{\partial t'}(\rho' h') + \alpha^2\frac{\partial}{\partial x'}(\rho' q') = 0 \qquad (4)$$

$$\frac{\partial}{\partial t'}(\rho' q') + \frac{\partial}{\partial x'}(\rho' h') - \theta\rho' h' + \nu\rho' q' - \rho' S_0' = 0 \qquad (5)$$

$\alpha = (T/L)\sqrt{gH}$ is a dimensionless measure of the wave speed $\sqrt{gH}$. It is also the ratio of the wave length to channel length, $\theta = \frac{1}{2}(L/\varrho_f)\ (\partial\varrho/\partial x)$ is a dimensionless measure of the longitudinal density gradient; $\nu = \mu T$ represents the influence of friction and $S_o' = (L/H)\ S_o$ is a measure of the bed slope.

Analytical Evaluation

For this study, a constant longitudinal density gradient is assumed. In real estuaries density varies with time but primarily with location. The constant value here can be approximated as the time-averaged value of the average longitudinal density gradient.

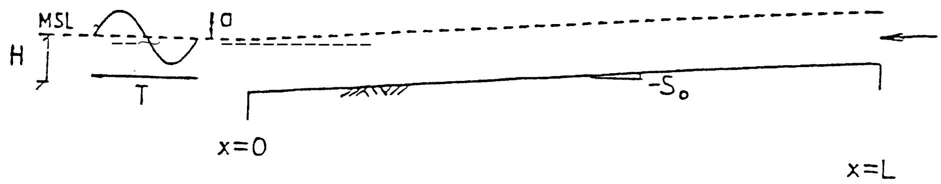

Fig. 1. Prototype Problem.

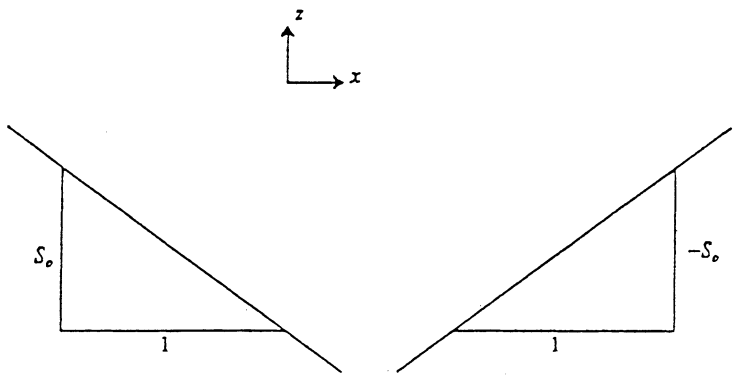

Fig. 2. Definition of bed slope.

The Prototype Problem

The prototype problem to be considered is as in Fig. 1. This consists of a wide rectangular channel with constant bottom slope S_o subject to at tide at $x = 0$

$$h(x=0, t) = H + a\sin\left(\frac{2\pi t}{T}\right)$$

where a is the wave amplitude and T the period. The definition of bed slope is illustrated in Fig. 2. Two types of specifications of boundary conditions will be considered at $x = L$;

1) Type 1 – specification of discharge $q(x=L, t) = q_u = constant$
2) Type 2 – specification of water depth $h(x=L, t) = H$

Because Eqs. (4) and (5) are linear, superposition of the solutions is valid. The complete solution to a problem will be separated into a steady (time-independent) component and a transient or forced (time-dependent) component. Each component can be considered separately. Furthermore, by change of variables x to L-x, solutions for the case where the tide is located at $x=L$ can be directly obtained from the solutions to this prototype problem. By superposition, any complicated set of boundary conditions at both ends which can be harmonically decomposed can be handled.

Let subscript s denote the steady response solution and subscript f denote the forced response solution and

$$h'(x,t) = h'_s(x) + h'_f(x,t) \quad , \quad q'(x,t) = q'_s(x) + q'_f(x,t)$$

Substitution in mass conservation Eq. (4) and momentum conservation Eq. (5) yields respectively for *steady response*

$$\alpha^2 \frac{\partial}{\partial x'}(\rho' q'_s) \equiv 0 \quad i.e. \quad \rho' q'_s = \text{constant} \tag{6}$$

$$\frac{d}{dx'}(\rho' h'_s) - \theta\rho' h'_s + \nu\rho' q'_s - \rho' S'_0 = 0 \tag{7}$$

subject to $h_s(0) = H$ *i.e.* $h'_s(0) = 1$. In addition, for discharge boundary condition upstream (type 1), $q_s(L) = q_u$ which implies $q'_s(1) = q_u L/gTH^2$, q_u will here be chosen to correspond to constant density uniform flow. For height boundary condition upstream (type 2), $h_s(L) = H$ *i.e.* $h'_s(1) = 1$.

For *forced response*

$$\frac{\partial}{\partial t'}(\rho' h'_f) + \alpha^2 \frac{\partial}{\partial x'}(\rho' q'_f) \equiv 0 \tag{8}$$

$$\frac{\partial}{\partial t'}(\rho' q'_f) + \frac{\partial}{\partial x'}(\rho' h'_f) - \theta\rho' h'_f + \nu\rho' q'_f = 0 \tag{9}$$

subject to

$$h_f(0,t) = a\sin(2\pi\frac{t}{T}) \quad ie \quad h'_f(0,t') = a'\sin(2\pi t) \qquad \text{where } a' = \frac{a}{H}$$

In addition for discharge boundary condition upstream (type 1)

$$q_f(L,t) = 0 = q'_f(1,t')$$

and for height boundary condition upstream (type 2), $h_f(L, t) = 0 = h'_f(1, t')$. As discussed earlier, a linear density distribution $\varrho(x) = \varrho_f - 2\theta\varrho_f\,(L\text{-}x)/L$ such that $\varrho(L) = \varrho_f$ and $\theta = ½(L/\varrho_f)\,(\partial\varrho/\partial x)$ (as already defined in the previous section) is assumed. This implies

$$\rho'(x') \equiv \frac{\rho(x'L)}{\rho_f} \equiv 1 - 2\theta(1-x') \tag{10}$$

Steady Response Effects

Dropping primes from all variables except the dependent variables h and q (because there is still need to refer to the dimensional values of h and q), the steady state solutions (from Eqs. (6) and (7)) are as follows:

Discharge Boundary Condition Upstream (Type 1)

For the case where $\theta = 0$ (*i.e.* no density gradient),

$$h_s'(x) = 1 \quad , \quad q_s'(x) = \frac{S_0}{\nu} \tag{11}$$

For $\theta \neq 0$, let $C = 1 - 2\theta + (2S_o/\theta)(1-\theta)$, then

$$h_s'(x) = \frac{1}{1-2\theta(1-x)}\left(2S_0 + C\exp(\theta x) + \frac{2S_0}{\theta}(-\theta x - 1)\right) \tag{12a}$$

$$q_s'(x) = \frac{S_0}{\nu(1-2\theta(1-x))} \tag{12b}$$

Eqs. (11) and (12) give an estimate of the impact of a constant longitudinal density gradient on the steady response. Let $\Delta(\Lambda)$ be the maximum absolute error over x (space) in any variable Λ due to the exclusion of longitudinal density gradient in calculations, then

$$\Delta(h_s') = \frac{\Delta(h_s)}{H} = \text{function}(\theta, S_0) \tag{13}$$

$$\Delta(\nu q_s') \equiv \frac{\Delta(q_s)\mu L}{gH^2} \equiv \text{function}(\theta, S_0) \tag{14}$$

The density of very saline ocean water (40 parts per thousand) at 4°C is about 1,032 kg/m^3. Thus the magnitude of θ could be as high as

$$\theta = \frac{1}{2}\frac{L}{\rho_f}\frac{\partial\rho}{\partial x} \approx \frac{1}{2}\frac{L}{1000}\frac{\Delta\rho}{L} \approx \frac{1}{2}\frac{32}{1000} \equiv 0.016$$

θ will be allowed to range from -0.02 to 0.02. Usually in estuaries bed slopes would not exceed 10^{-3}, L of 20 km is quite long and H of 2 m is relatively shallow implying a maximum magnitude of $S_o' = 10$. Thus S_o' will be allowed to range from -10 to 10.

The dependence of $\Delta(h_s')$ and $\Delta(\nu q_s')$ on S_o' and θ for discharge boundary condition upstream are respectively as in Tables 1a and b. These show approximate symmetry of the contours with respect to $\theta = 0$ and $S_o' = 0$. The errors generally increase with increasing magnitudes of θ and S_o'. The non-dimensionalization done earlier implies

$$\Delta(h_s) = \Delta(h_s')H \quad ; \quad \Delta(q_s) = \frac{gH^2}{\mu L}\Delta(\nu q_s') \tag{15}$$

where μ the linear friction coefficient can be estimated from

$$\mu \equiv \frac{g|v|}{C^2R} \equiv \frac{gn^2|v|}{R^{4/3}} \tag{16}$$

$|v|$ is an effective mean of the absolute values of the velocities, C is Chezy's friction coefficient, R the hydraulic radius and n is Manning's friction coefficient. For a purely sinusoidal flow, $|v|$ has been estimated using Lorentz's energy dissipation

Table 1a – Dimensionless steady errors in head $\triangle(h_s')$ for discharge boundary condition upstream.

S_o''	θ values										
	-.02	-.016	-.012	-.008	-.004	.0	.004	.008	.012	.016	.02
-10	1.8E-1	1.4E-1	1.1E-1	7.2E-2	3.6E-2	1.9E-6	3.6E-2	7.3E-2	1.1E-1	1.5E-1	1.8E-1
-8	1.4E-1	1.1E-1	8.4E-2	5.6E-2	2.8E-2	1.9E-6	2.8E-2	5.7E-2	8.5E-2	1.1E-1	1.4E-1
-6	1.0E-1	8.0E-2	6.0E-2	4.0E-2	2.0E-2	1.5E-8	2.0E-2	4.1E-2	6.1E-2	8.1E-2	1.0E-1
-4	6.1E-2	4.9E-2	3.7E-2	2.4E-2	1.2E-2	9.6E-7	1.2E-2	2.5E-2	3.7E-2	4.9E-2	6.2E-2
-2	2.2E-2	1.8E-2	1.3E-2	9.0E-3	4.5E-3	4.8E-7	4.5E-3	9.0E-3	1.4E-2	1.8E-2	2.3E-2
0	1.9E-2	1.6E-2	1.2E-2	7.9E-3	4.0E-3	1.4E-9	4.0E-3	8.1E-3	1.2E-2	1.6E-2	2.1E-2
2	5.9E-2	4.7E-2	3.6E-2	2.4E-2	1.2E-2	4.8E-7	1.2E-2	2.4E-2	3.6E-2	4.9E-2	6.1E-2
4	9.8E-2	7.9E-2	5.9E-2	4.0E-2	2.0E-2	9.7E-7	2.0E-2	4.0E-2	6.1E-2	8.1E-2	1.0E-1
6	1.4E-1	1.1E-1	8.3E-2	5.6E-2	2.8E-2	1.9E-8	2.8E-2	5.6E-2	8.5E-2	1.1E-1	1.4E-1
8	1.8E-1	1.4E-1	1.1E-1	7.2E-2	3.6E-2	1.9E-6	3.6E-2	7.2E-2	1.1E-1	1.5E-1	1.8E-1
10	2.2E-1	1.7E-1	1.3E-1	8.7E-2	4.4E-2	1.9E-6	4.4E-2	8.9E-2	1.3E-1	1.8E-1	2.2E-1

Table 1b – Dimensionless steady errors in discharge $\triangle(\nu q_s')$ for discharge boundary condition upstream.

S_o''	θ values										
	-.02	-.016	-.012	-.008	-.004	.0	.004	.008	.012	.016	.02
-10	3.8E-1	3.1E-1	2.3E-1	1.6E-1	7.9E-2	2.8E-8	8.1E-2	1.6E-1	2.5E-1	3.3E-1	4.2E-1
-8	3.1E-1	2.5E-1	1.9E-1	1.3E-1	6.3E-2	2.2E-8	6.5E-2	1.3E-1	2.0E-1	2.6E-1	3.3E-1
-6	2.3E-1	1.9E-1	1.4E-1	9.4E-2	4.8E-1	1.7E-8	4.8E-2	9.8E-2	1.5E-1	2.0E-1	2.5E-1
-4	1.5E-1	1.2E-1	9.4E-2	6.3E-2	3.2E-2	1.1E-8	3.2E-2	6.5E-2	9.8E-2	1.3E-1	1.7E-1
-2	7.7E-2	6.2E-2	4.7E-2	3.1E-2	1.6E-2	5.6E-9	1.6E-2	3.3E-2	4.9E-2	6.6E-2	8.3E-2
0	0	0	0	0	0	0	0	0	0	0	0
2	7.7E-2	6.2E-2	4.7E-2	3.1E-2	1.6E-2	5.6E-9	1.6E-2	3.3E-2	4.9E-2	6.6E-2	8.3E-2
4	1.5E-1	1.2E-1	9.4E-2	6.3E-2	3.2E-2	1.1E-8	3.2E-2	6.5E-2	9.8E-2	1.3E-1	1.7E-1
6	2.3E-1	1.9E-1	1.4E-1	9.4E-2	4.8E-2	1.7E-8	4.8E-2	9.8E-2	1.5E-1	2.0E-1	2.5E-1
8	3.1E-1	2.5E-1	1.9E-1	1.3E-1	6.3E-2	2.2E-8	6.5E-2	1.3E-1	2.0E-1	2.6E-1	3.3E-1
10	3.8E-1	3.1E-1	2.3E-1	1.6E-1	7.9E-2	2.8E-8	8.1E-2	1.6E-1	2.5E-1	3.3E-1	4.2E-1

argument (Dronkers 1964) as $|v| = 8U_m/3\pi$, where U_m is the velocity amplitude.

Errors in velocity rather than in q are more appropriate and the dimensional error in velocity from steady response $\triangle(u_s) \approx \triangle(q_s)/H$, *i.e.* from Eq. (15)

$$\Delta(u_s) \approx \frac{gH}{\mu L}\Delta(\nu q_s') \tag{17}$$

Substituting Eq. (16) in (17), with $R \approx H$

$$\Delta(u_s) \approx \frac{H^{7/3}}{Ln^2|v|}\Delta(\nu q_s') \tag{18}$$

Table 1c – Dimensionless steady errors in head $\triangle(h_s')$ for head boundary condition upstream.

S_o'	θ values										
	-.02	-.016	-.012	-.008	-.004	.0	.004	.008	.012	.016	.02
-10	4.9E-2	3.9E-2	3.0E-2	2.0E-2	1.0E-2	1.6E-6	1.0E-2	2.0E-2	3.0E-2	4.1E-2	5.1E-2
-8	3.9E-2	3.2E-2	2.4E-2	1.6E-2	8.0E-3	1.3E-6	8.0E-3	1.6E-2	2.4E-2	3.2E-2	4.1E-2
-6	3.0E-2	2.4E-2	1.8E-2	1.2E-2	6.0E-3	9.4E-7	6.0E-3	1.2E-2	1.8E-2	2.4E-2	3.1E-2
-4	2.0E-2	1.6E-2	1.2E-2	8.0E-3	4.0E-3	6.3E-7	4.0E-3	8.0E-3	1.2E-2	1.6E-2	2.0E-2
-2	9.9E-3	7.9E-3	6.0E-3	4.0E-3	2.0E-3	3.1E-7	2.0E-3	4.0E-3	6.0E-3	8.1E-3	1.0E-2
0	9.8E-5	6.3E-5	3.6E-5	1.6E-5	4.0E-6	2.2E-16	4.0E-6	1.6E-5	3.6E-5	6.5E-5	1.0E-4
2	9.7E-3	7.8E-3	5.9E-3	4.0E-3	2.0E-3	3.1E-7	2.0E-3	4.0E-3	6.1E-3	8.2E-3	1.0E-2
4	2.0E-2	1.6E-2	1.2E-2	7.9E-3	4.0E-3	6.3E-7	4.0E-3	8.1E-3	1.2E-2	1.6E-2	2.1E-2
6	2.9E-2	2.4E-2	1.8E-2	1.2E-2	6.0E-3	9.4E-7	6.0E-3	1.2E-2	1.8E-2	2.4E-2	3.1E-2
8	3.9E-2	3.1E-2	2.4E-2	1.6E-2	8.0E-3	1.3E-6	8.0E-3	1.6E-2	2.4E-2	3.3E-2	4.1E-2
10	4.9E-2	3.9E-2	3.0E-2	2.0E-2	1.0E-2	1.6E-6	1.0E-2	2.0E-2	3.0E-2	4.1E-2	5.1E-2

Table 1d – Dimensionless steady errors in discharge $\triangle(\nu q_s')$ for head boundary condition upstream.

S_o'	θ values										
	-.02	-.016	-.012	-.008	-.004	.0	.004	.008	.012	.016	.02
-10	2.1E-1	1.7E-1	1.3E-1	8.7E-2	4.4E-2	2.7E-8	4.4E-2	8.9E-2	1.4E-1	1.8E-1	2.3E-1
-8	1.7E-1	1.4E-1	1.1E-1	7.1E-2	3.6E-2	2.1E-8	3.6E-2	7.3E-2	1.1E-1	1.5E-1	1.9E-1
-6	1.3E-1	1.1E-1	8.2E-2	5.5E-2	2.8E-2	1.5E-8	2.8E-2	5.7E-2	8.6E-2	1.2E-1	1.5E-1
-4	9.6E-2	7.7E-2	5.9E-2	3.9E-2	2.0E-2	9.8E-9	2.0E-2	4.1E-2	6.2E-2	8.3E-2	1.0E-1
-2	5.7E-2	4.6E-2	3.5E-2	2.4E-2	1.2E-2	4.2E-9	1.2E-2	2.4E-2	3.7E-2	5.0E-2	6.3E-2
0	2.0E-2	1.6E-2	1.2E-2	7.9E-3	4.0E-3	1.4E-9	4.0E-3	8.2E-3	1.2E-2	1.7E-2	2.1E-2
2	5.9E-2	4.8E-2	3.6E-2	2.4E-2	1.2E-2	7.0E-9	1.2E-2	2.4E-2	3.6E-2	4.8E-2	6.1E-2
4	9.9E-2	8.0E-2	6.0E-2	4.0E-2	2.0E-2	1.3E-8	2.0E-2	4.0E-2	6.0E-2	8.0E-2	1.0E-1
6	1.4E-1	1.1E-1	8.4E-2	5.6E-2	2.8E-2	1.8E-8	2.8E-2	5.6E-2	8.4E-2	1.1E-1	1.4E-1
8	1.8E-1	1.4E-1	1.1E-1	7.2E-2	3.6E-2	2.4E-8	3.6E-2	7.2E-2	1.1E-1	1.4E-1	1.8E-1
10	2.2E-1	1.8E-1	1.3E-1	8.8E-2	4.4E-2	2.9E-8	4.4E-2	8.8E-2	1.3E-1	1.8E-1	2.2E-1

For a moderate value of $\triangle(h_s')$ of 0.02, from Table 1a, $\triangle(h_s)$ would vary from 0.04 m in a depth of 2 m to 0.4 m in a depth of 20 m. For moderate values of depth H = 5 m, L = 5 km, n = 0.04, $|v|$ = 0.5 m/s and $\triangle(\nu q_s')$ = 0.05 (from Table 1b); $\triangle(u_s)$ = 0.53 m/s. These estimates for $\triangle(h_s)$ and $\triangle(u_s)$ suggest that longitudinal density gradients may have a significant impact for discharge boundary condition upstream. This is further discussed after the numerical evaluation.

Height Boundary Condition Upstream (Type 2)

The governing equation and boundary conditions are as earlier defined. For $\theta \neq 0$

$$h_s'(x) = \frac{1}{1-2\theta(1-x)}(\gamma - \frac{S_0}{\theta}(1-2\theta)+C\exp(\theta x)+\frac{2S_0}{\theta}(-\theta x-1)) \quad (19)$$

$$q_s'(x) = \frac{\gamma\theta}{(1-2\theta(1-x))\nu} \quad (20)$$

where $C \equiv (2\theta + 2S_o)/(\exp(\theta)-1)$ and $\gamma \equiv 1-2\theta + S_o/\theta\,(1\text{-}2\theta + 2S_o/\theta - C$. For $\theta =$ 0,

$$h_s'(x) = 1 \;, \qquad q_s'(x) = \frac{S_0}{\nu}$$

The dependence of $\triangle(h_s')$ and $\triangle(\nu q_s')$ on S_o and θ for height boundary condition upstream are respectively as in Tables 1c and d. The values of $\triangle(h_s')$ are generally almost an order of magnitude less than corresponding values for discharge boundary condition upstream while the values of $\triangle(\nu q_s')$ are generally about a factor of 2 smaller than corresponding values for discharge boundary condition upstream. However for S_o' very close to zero, $\triangle(\nu q_s')$ values are generally larger than corresponding values for discharge boundary condition upstream. The same trends would apply to the dimensional errors too.

Forced Response Effects

Here it is convenient to neglect friction. This should not affect the results adversely. As friction has a dissipative effect, its neglect would tend to be conservative in estimating the errors. Dropping primes from *x, t* and ϱ terms, the forced response solutions are as follows:

In all cases, the solutions are of the form

$$h_f'(x,t) = \frac{a'(1-2\theta)}{1-2\theta(1-x)} f(x)\sin(2\pi t) \quad (21)$$

$$q_f'(x,t) = \frac{a'(1-2\theta)}{1-2\theta(1-x)} g(x)\cos(2\pi t) \quad (22)$$

The values of $f(x)$ and $g(x)$ are defined as follows:

Case 1 $\frac{\alpha\theta}{4\pi} < 1$

$$f(x) = \exp(\frac{\theta}{2}x)(\cos(\beta x)+d_2\sin(\beta x))$$

$$g(x) = \frac{1}{2\pi}\exp(\frac{\theta}{2}x)((\beta d_2-\frac{\theta}{2})\cos(\beta x)+(-\frac{\theta}{2}d_2-\beta)\sin(\beta x))$$

where

$$\beta = \left[\left[\frac{2\pi}{\alpha}\right]^2 - \left[\frac{\theta}{2}\right]^2\right]^{\frac{1}{2}}$$

$$d_2 \equiv \frac{\beta \sin(\beta) + \frac{\theta}{2}\cos(\beta)}{\beta\cos(\beta) - \frac{\theta}{2}\sin(\beta)}$$

for discharge boundary condition upstream (type 1) and

$$d_2 = -\cot(\beta)$$

for height boundary condition upstream (type 2).

Case 2 $\frac{\alpha\theta}{4\pi} \equiv 1$

$$f(x) \equiv \exp(\frac{\theta}{2}x) + d_2 x \ \exp(\frac{\theta}{2}x),$$

$$g(x) = \frac{1}{2\pi}(-\frac{\theta}{2}\exp(\frac{\theta}{2}x) + d_2(1-\frac{\theta}{2}x)(\exp(\frac{\theta}{2}x))$$

where

$$d_2 \equiv \frac{\theta}{2-\theta}$$

for discharge boundary condition upstream and

$$d_2 = -1$$

for height boundary condition upstream

Case 3 $\frac{\alpha\theta}{4\pi} > 1$

Let

$$\gamma_1 = \frac{\theta}{2} + \left[\left[\frac{\theta}{2}\right]^2 - \left[\frac{2\pi}{\alpha}\right]^2\right]^{\frac{1}{2}} \quad \text{and} \quad \gamma_2 = \frac{\theta}{2} - \left[\left[\frac{\theta}{2}\right]^2 - \left[\frac{2\pi}{\alpha}\right]^2\right]^{\frac{1}{2}}$$

then

$$f(x) = d_1\exp(\gamma_1 x) + d_2\exp(\gamma_2 x)$$

$$g(x) \equiv \frac{1}{2\pi}(d_1(\gamma_1 - \theta)\exp(\gamma_1 x) + d_2(\gamma_2 - \theta)\exp(\gamma_2 x))$$

where

$$d_1 \equiv \frac{-\exp(\gamma_2)(\gamma_2 - \theta)}{\exp(\gamma_1)(\gamma_1 - \theta) - \exp(\gamma_2)(\gamma_2 - \theta)}$$

for discharge boundary condition upstream (type 1) and

$$d_1 \equiv \frac{-\exp(\gamma_2)}{\exp(\gamma_1) - \exp(\gamma_2)}$$

for height boundary condition upstream. $d_2 = 1 - d_1$ in both cases.

The errors due to forced response for a given θ are obtained by taking the difference between the h_f' and q_f' values obtained using θ in the above equations and the corresponding values obtained when $\theta = 0$. The errors are also periodic with maximum error magnitudes for h_f' occurring at $t = 1/4$ and $t\,3/4$ and for q_f' at $t = 0$ and $t \equiv 1/2$ at any x. Here let $\triangle(\Lambda)$ be the maximum magnitude over x and t of the errors in any variable Λ, values of $\triangle(h_f'/a')$ and $\triangle(q_f'/a')$ are as in Tables 2a and b respectively for discharge boundary condition upstream. Both tables show almost exact symmetry with respect to $\theta = 0$. $\triangle(h_f'/a')$ also shows strong dependence on θ but relatively little dependence on α. $\triangle(q_f'/a')$ is however strongly dependent on both α and θ with the errors generally increasing with the magnitude of θ and decreasing with α. Now

$$\Delta\left(\frac{h_f'}{a'}\right) = \frac{\Delta(h_f)/H}{a/H} = \frac{\Delta(h_f)}{a}; \quad \Delta\left(\frac{q_f'}{a'}\right) = \frac{\Delta(q_f)L/gTH^2}{a/H} = \frac{\Delta(q_f)L}{gTHa} \tag{23}$$

Using $\triangle(q_f) \approx \triangle(u_f)H$, where u_f is the velocity due to forced response, then

$$\Delta\left(\frac{q_f'}{a'}\right) \doteq \frac{\Delta(u_f)L}{gTa} \tag{24}$$

For $\triangle(h_f'/a') = 0.008$ from Table 2a and a typical value of $a = 1$ m, $\triangle(h_f) = 0.008$ m. For $\triangle(q_f'/a') = 10^{-4}$ (Table 2b), $T = 12.5$ hours, $a = 1$ m and a moderate $L = 5$ km, $\triangle(u_f) = 0.009$ m/s. These estimates tend to suggest that the errors due to forced response are negligible.

For height boundary condition upstream, values of $\triangle(h_f'/a')$ and $\triangle(q_f'/a')$ are as in Tables 2c and d respectively. Both tables again show near perfect symmetry relative to $\theta = 0$ and relative independence of α. The values of $\triangle(h_f'/a')$ are generally about a factor of 2 less than corresponding values for discharge boundary condition upstream while the values of $\triangle(q_f'/a')$ are quite often several orders of magnitude larger than corresponding values for discharge boundary condition upstream especially for large values of α.

Numerical Evaluation of Longitudinal Density Gradient Effects on Hydrodynamics

To validate the ability of the analysis presented earlier to predict the errors arising from the exclusion of longitudinal density gradient effects in actual numerical computations, two sets of numerical experiments were designed. The first set of numerical experiments was designed to violate the assumptions made in setting up the steady response and transient response problems as much as possible while the second set was designed to be closely consistent with the assumptions. The specific parameters for the experiments are in Table 3a. The first involves a relatively large forcing amplitude 1 m in shallow water of depth 2 m thus significantly violating

Table 2a - Dimensionless unsteady errors in head $\triangle(h_f'/a')$ for discharge boundary condition upstream.

$Log_{10}(\alpha^2)$	θ values										
	-.02	-.016	-.012	-.008	-.004	.0	.004	.008	.012	.016	.02
1.5	2.5E-2	2.0E-2	1.5E-2	1.0E-2	5.3E-3	1.9E-9	5.4E-3	1.1E-2	1.6E-2	2.2E-2	2.8E-2
2.5	2.0E-2	1.6E-2	1.2E-2	8.2E-3	4.1E-3	1.5E-9	4.2E-3	8.4E-3	1.3E-2	1.7E-2	2.2E-2
3.5	1.9E-2	1.6E-2	1.2E-2	7.9E-3	4.0E-3	1.4E-9	4.0E-3	8.1E-3	1.2E-2	1.6E-2	2.1E-2
4.5	1.9E-2	1.6E-2	1.2E-2	7.9E-3	4.0E-3	1.4E-9	4.0E-3	8.1E-3	1.2E-2	1.6E-2	2.1E-2
5.5	1.9E-2	1.6E-2	1.2E-2	7.9E-3	4.0E-3	1.4E-9	4.0E-3	8.1E-3	1.2E-2	1.6E-2	2.1E-2

Table 2b - Dimensionless unsteady errors in discharge $\triangle(q_f'/a')$ for discharge boundary condition up stream.

$Log_{10}(\alpha^2)$	θ values										
	-.02	-.016	-.012	-.008	-.004	.0	.004	.008	.012	.016	.02
1.5	6.6E-3	5.3E-3	4.0E-3	2.7E-3	1.3E-3	4.7E-10	1.3E-3	2.7E-3	4.1E-3	5.4E-3	6.8E-3
2.5	2.1E-4	1.7E-4	1.3E-4	8.6E-5	4.3E-5	1.5E-11	4.3E-5	8.7E-5	1.3E-4	1.7E-4	2.2E-4
3.5	2.0E-5	1.6E-5	1.2E-5	8.0E-6	4.0E-6	1.4E-12	4.0E-6	8.0E-6	1.2E-5	1.6E-5	2.0E-5
4.5	2.0E-6	1.6E-6	1.2E-6	7.9E-7	4.0E-7	1.4E-13	4.0E-7	8.0E-7	1.2E-6	1.6E-6	2.0E-6
5.5	2.0E-7	1.6E-7	1.2E-7	7.9E-8	4.0E-8	1.4E-14	4.0E-8	8.0E-8	1.2E-7	1.6E-7	2.0E-7

Table 2c – Dimensionless unsteady errors in head $\triangle(h'_f/a')$ for head boundary condition upstream.

$Log_{10}(\alpha^2)$	θ values										
	-.02	-.016	-.012	-.008	-.004	.0	.004	.008	.012	.016	.02
1.5	8.6E-3	6.9E-3	5.2E-3	3.5E-3	1.8E-3	6.2E-10	1.8E-3	3.6E-3	5.4E-3	7.3E-3	9.2E-3
2.5	7.4E-3	5.9E-3	4.5E-3	3.0E-3	1.5E-3	5.3E-10	1.5E-3	3.1E-3	4.7E-3	6.3E-3	7.9E-3
3.5	7.3E-3	5.9E-3	4.4E-3	3.0E-3	1.5E-3	5.2E-10	1.5E-3	3.0E-3	4.6E-3	6.2E-3	7.8E-3
4.5	7.3E-3	5.8E-3	4.4E-3	3.0E-3	1.5E-3	5.2E-10	1.5E-3	3.0E-3	4.6E-3	6.2E-3	7.8E-3
5.5	7.3E-3	5.8E-3	4.4E-3	3.0E-3	1.5E-3	5.2E-10	1.5E-3	3.0E-3	4.6E-3	6.2E-3	7.8E-3

Table 2d – Dimensionless unsteady errors in discharge $\triangle(q'_f/a')$ for head boundary conditions upstream.

$Log_{10}(\alpha^2)$	θ values										
	-.02	-.016	-.012	-.008	-.004	.0	.004	.008	.012	.016	.02
1.5	5.9E-3	4.7E-3	3.5E-3	2.4E-3	1.2E-3	4.1E-10	1.2E-3	2.4E-3	3.6E-3	4.8E-3	6.0E-3
2.5	4.8E-3	3.9E-3	2.9E-3	1.9E-3	9.7E-4	3.4E-10	9.8E-4	2.0E-3	2.9E-3	3.9E-3	4.9E-3
3.5	4.7E-3	3.8E-3	2.8E-3	1.9E-3	9.5E-4	3.3E-10	9.6E-4	1.9E-3	2.9E-3	3.9E-3	4.8E-3
4.5	4.7E-3	3.8E-3	2.8E-3	1.9E-3	9.5E-4	3.3E-10	9.6E-4	1.9E-3	2.9E-3	3.9E-3	4.8E-3
5.5	4.7E-3	3.8E-3	2.8E-3	1.9E-3	9.5E-4	3.3E-10	9.6E-4	1.9E-3	2.9E-3	3.9E-3	4.8E-3

Table 3a – Parameters used in the numerical evaluation of the effect of longitudinal density gradient on estuarine hydrodynamics

Test No.	$H(m)$	$a(m)$	$L(km)$	n	S_o	α	S_o'
1	2.0	1.0	10.0	0.029	0.	19.92	0.
2	20.0	1.0	10.0	0.034	0.001	63.01	0.5

Table 3b – Numerically computed errors in head due to the exclusion of longitudinal density gradient

Test	B.C.	Errors in head $\triangle(h)$ (m)			
No.	type		Analytical		Numerical
		Steady	Forced	Total	
1	1	2.93E-2	1.52E-2	4.45E-2	3.07E-2
	2	1.11E-4	5.56E-3	5.67E-3	1.29E-2
2	1	1.45E-1	1.50E-2	1.60E-1	1.34E-1
	2	3.80E-2	5.50E-3	4.35E-2	1.08E-1

Table 3c – Numerically computed errors in velocity due to the exclusion of longitudinal density gradient

Test	B.C.	Errors in velocity $\triangle(u)$ (m/s)			
No.	type		Analytical		Numerical
		Steady	Forced	Total	
1	1	0.	5.60E-3	5.60E-3	3.52E-2
	2	4.92E-2	1.59E-1	2.08E-1	3.44E-2
2	1	1.97E-1	5.24E-4	1.98E-1	2.13E-1
	2	2.92E-1	1.57E-1	4.48E-1	1.88E-1

assumption 2 (p. 67). Because of the shallow depth, the wave speed and hence the wave length would be small implying a rapid variation in the variables h and q with respect to distance. The convective acceleration term might thus be important, violating assumption 1. The bed slope was set to zero implying there is insignificant throughflow and hence the flow would tend to reverse strongly, violating assumption 4 (linear friction). The second set was based on opposite considerations to above with the forcing amplitude remaining at 1 m in a water depth of 20 m. Bed slope was set to a relatively large value of 0.001.

For the numerical experiments, Program ESTFLO developed by Sobey *et al.* (1980) for solving the one-dimensional, constant density, hydrodynamics equations in channel networks was adapted (Aiyesimoju 1986) to optionally include longitudinal density gradient effects. ESTFLO uses an implicit, space but not time stagered grid of head and discharge. For Courant Numbers ($c(\triangle t/\triangle x)$ where c is wave speed) less than about 4 and $L/\triangle x$ (where L is wave length) greater than about 20 which are typical in estuarine hydrodynamics, the results are highly satisfactory.

The results obtained from the numerical experiments and the corresponding analytical results are as in Tables 3b and c for errors in head and errors in velocity respectively. The test parameters are summarized in Table 3a. As expected, the set 2 experiments errors are better predicted, all being within a factor of 2.5. The set 1 errors were all predicted within a factor of 6. Other experiments were performed which confirmed this range of accuracy in the prediction of errors due to exclusion of longitudinal density gradient effects from hydrodynamics computations.

Error Analysis and Discussion

To give further perspective to the range of errors that could occur, analytically predicted errors were computed for combinations of flow depths ranging from 2 m to 20 m, channel lengths from 2 km to 20 km, Manning's roughnes coefficients from 0.02 to 0.04 and bed slopes from 0 to 0.001. θ was set to 0.015, the tidal amplitude a to 1 m and the tidal period T to 12.5 hours.

These calculations show that in general, errors in velocity stem predominantly from the steady response. Also, in general, the largest errors in velocity occur for large longitudinal density gradient, short channel, deep water, low friction and height boundary condition upstream (type 2). For discharge boundary condition upstream, the larger the bed slope, the larger the errors in velocity while for height boundary condition upstream, the errors in velocity are not so dependent on the bed slope.

Longitudinal density gradient in estuaries is normally the result of fresh water inflow at estuary head. This freshwater inflow also usually serves as boundary condition for hydrodynamic simulations. The other boundary condition is usually water level at the mouth of the estuary. Thus substantial longitudinal density gradient would usually go with discharge boundary condition upstream. As it is rare to have a short estuary which is very deep, the large errors that might arise in short estuaries would tend to be moderated by their shallowness and conversely the large errors that might arise in deep estuaries would tend to be moderated by their length. Additional numerical computations confirm this for a short channel of length 2 km and water depth of 2 m and a long channel of length 20 km and water depth 20 m. The errors in the velocity in these cases were no more than order 10^{-2}m/s for $\theta = 0.015$. On the other hand, for the rare situation of channel length 2 km and depth 20 m, errors up to 2 m/s were obtained even for a Manning's n of up to 0.04.

The errors in head when significant (greater than 0.1 m) occurred for discharge boundary condition (Type 1) and stemmed mainly from the steady response.

Conclusions

The impact of longitudinal density gradients when significant is primarily due to the steady response and varies widely depending on channel length, bed slope, bottom friction, water depth, boundary condition type and of course longitudinal density gradient. The analysis presented predicted these errors from near exactly in the best cases to within a factor of 6 in the worst cases. The equations developed should thus be useful for at least an order of magnitude estimation of the impact of longitudinal density gradients that takes all the relevant parameters into account.

References

Aiyesimoju, K.O. (1986) Numerical prediction of transient water quality in estuarine/river networks, Hydraulic Eng. Lab. Report UCB/HEL-86/06, Univ of California, Berkeley.

Bode, L., and Sobey, R.J. (1984) Initial transients in long wave computations, *Journal of Hydraulic Engineering, ASCE, Vol. 110,* pp. 1371-1397.

Dronkers, J.J. (1964) *Tidal computations in rivers and coastal waters,* North Holland, Amsterdam.

Dailey, J.E., and Harleman, D.R.F. (1972) A numerical model for the prediction of transient water quality in estuary networks, Report No. 158, Ralph M. Parsons Lab., M.I.T.

Fisher, J.S., Nava, R.E., and Cross, R.H. (1971) Mathematical model of the Maracaibo estuary, Report No. 136, Ralph M. Parsons Lab., M.I.T.

Liu, S.K., and Leendertsee, J.J. (1978) Multi-dimensional numerical modeling, *Advances in Hydrosciences, Vol. 11,* pp. 95-165.

Sobey, R.J., Vidler, T.S., and Vidler, P.F. (1980) Users Guide to ESTFLO/Version: 2B, Dept. of Civil and Systems Eng., James Cook Univ., Townsville, Australia, Res. Bulletin No. CS 22.

TRACOR Inc. (1971) Estuary Modeling: An Assessment, Water Quality Office, Environmental Protection Agency.

Received: 6 June, 1989
Revised version received: 12 September, 1989
Accepted: 16 September, 1989

Address:
1528 Alice, No. 12,
Oakland, CA-94612, U.S.A.